PERIOD-N BIFURCATIONS IN MILLING: NUMERICAL AND EXPERIMENTAL VERIFICATION

Andrew Honeycutt and Tony L. Schmitz
Department of Mechanical Engineering and Engineering Science
University of North Carolina at Charlotte
Charlotte, NC

INTRODUCTION

Many years of machining simulation and measurement research have led to a comprehensive understanding of milling process dynamics. As early as 1946 Arnold studied chatter in steel machining [1]. Doi and Kato described self-excited vibrations using time-delay differential equations in 1956 [2]. During this time, the notion of "regeneration of waviness" was promoted as the feedback mechanism (time-delay term), where the previously cut surface combined with the instantaneous vibration state dictates the current chip thickness, force level, and corresponding vibration response [3-5]. This work resulted in analytical algorithms that were used to produce the now well-known stability lobe diagram that separates the spindle speed-chip width domain into regions of stable and unstable behavior.

Time domain simulation offers a powerful tool for exploring milling behavior and has been applied to identify instability [6]. For example, Zhao and Balachandran implemented a time domain simulation which incorporated loss of tool-workpiece contact and regeneration to study milling [7]. They identified secondary Hopf bifurcation and suggested that "period-doubling bifurcations are believed to occur" for low radial immersions. They included bifurcation diagrams for limited axial depth of cut ranges at two spindle speeds to demonstrate the two bifurcation types.

The semi-discretization, time finite element analysis, and multi-frequency methods were also developed to produce milling stability charts that demonstrate both instabilities [8]. In [9], it was shown using the semi-discretization method that the period-2 bifurcation exhibits closed, lens-like, curves within the secondary Hopf lobes, except for the highest speed stability lobe. The same group reported further experimental evidence of quasi-periodic (secondary Hopf), period-2, period-3, period-4, and combined quasi-periodic and period-2 chatter, depending on the spindle speed-axial depth values for a two degree of freedom dynamic system [9].

In this paper, period-n bifurcations are experimentally identified for n = 2, 3, 6, 7, and 15. Additionally, the sensitivity of the bifurcation behavior to system dynamics, including both natural frequency and damping, is explored. A comparison of numerical simulation predictions and experiments is presented.

POINCARÉ MAPS

In this study, Poincaré maps were developed using both experiments and simulations. For the experiments, the displacement and velocity of a flexible workpiece were recorded and then sampled once per tooth period. In simulation, the displacement and velocity were predicted, but the same sampling strategy was applied. By plotting the displacement versus velocity, the phase space trajectory can be observed in both cases. The once per tooth period samples are then superimposed and used to interrogate the milling process behavior. For stable cuts, the motion is periodic with the tooth period, so the sampled points repeat and a single grouping of points is observed. When secondary Hopf instability occurs, the motion is quasi-periodic with tool rotation because the chatter frequency is (generally) incommensurate with the tooth passing frequency. In this case, the once per tooth sampled points do not repeat and they form an elliptical distribution. For period-2 instability, on the other hand, the motion repeats only once every other cycle (i.e., it is a sub-harmonic of the forcing frequency). In this case, the once per tooth sampled points alternate between two solutions. For period-n instability, the sampled points appear at n locations.

TIME-DOMAIN SIMULATION

Time-domain simulation entails the numerical solution of the governing equations of motion for milling in small time steps [10]. It is well-suited to incorporating all the intricacies of milling dynamics, including the nonlinearity that occurs if the tooth leaves the cut due to large amplitude vibrations and complicated tool geometries (including runout, or different radii, of the cutter teeth, non-proportional teeth spacing, and variable helix).

Using the time-domain simulation approach, the forces and displacements may be calculated. These results are then once-per-tooth sampled to generate the Poincaré maps.

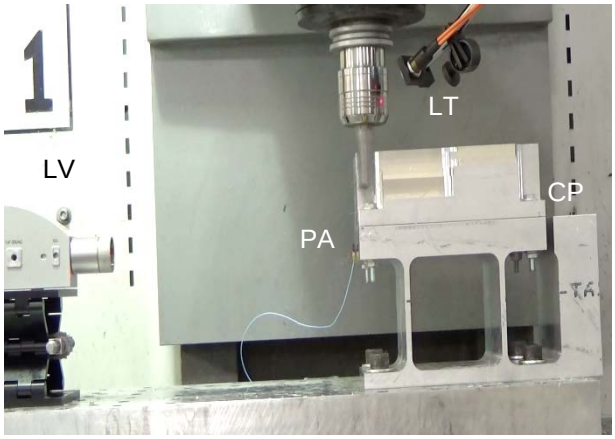

Figure 1. Milling experimental setup with laser vibrometer (LV), piezo-accelerometer (PA), laser tachometer (LT), and capacitance probe (CP).

Table 1. Cutting conditions and flexure dynamics for experiments.

	Cutting conditions		
Period-n	Spindle speed (rpm)	Axial depth, b (mm)	Radial depth (mm)
2	3486	2.0	1
3	3800	4.5	5
6	3200	18.0	1
6	3250	15.5	1
7	3200	14.5	1
15	3200	14.0	1
	Flexure dynamics		
Period-n	Stiffness (N/m)	Natural frequency (Hz)	Damping ratio (%)
2	9.0×10^5	83.0	2.00
3	5.6×10^6	163.0	1.08
6	5.6×10^6	202.6	0.28
6	5.6×10^6	205.8	0.28
7	5.6×10^6	204.1	0.28
15	5.6×10^6	204.8	0.28

RESULTS

A single degree of freedom (SDOF) flexure was used to define the system dynamics. Modal impact testing verified that the cutting tool dynamic stiffness (1055 Hz natural frequency, 0.045 viscous damping ratio, and 4.2×10^7 N/m stiffness) was much higher than the SDOF flexure. The flexure setup also simplified the measurement instrumentation. The flexure motions were measured using both a laser vibrometer and a low mass accelerometer. In order to enable once per tooth sampling of the vibration signals, a laser tachometer was used. A small section of reflective tape was attached to the tool and the corresponding laser tachometer signal used to perform the once per tooth sampling.

The cutting tool was a 20 mm diameter, single flute carbide square endmill. Modal impact testing verified that the cutting tool stiffness was much higher than the SDOF flexure. Each cut of the 6061-T6 aluminum workpiece was performed using a feed per tooth of 0.10 mm/tooth.

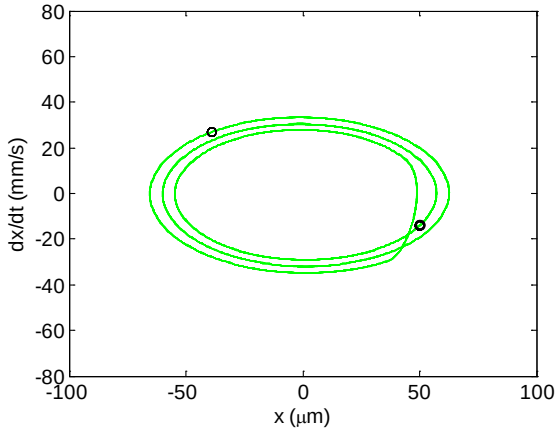

Figure 2(a). Poincaré map for simulated period-2 bifurcation.

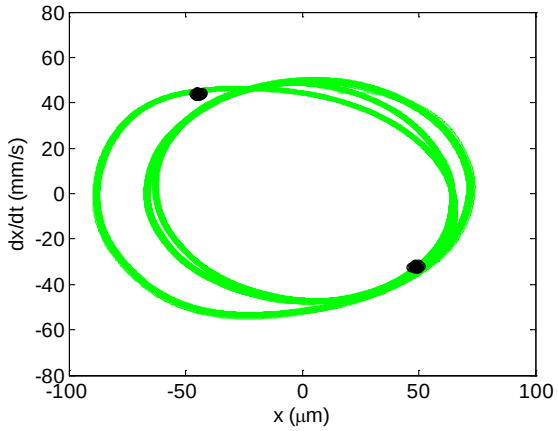

Figure 2(b). Poincaré map for experimental period-2 bifurcation.

Cutting tests were completed using the Fig. 1 setup. The measured flexure dynamics and cutting conditions are listed in Table 1. Results for period-2, 3, 6, 7, and 15 bifurcations are displayed in Figs. 2-7. In each figure, (a) shows the simulated behavior and

(b) shows the experimental result. Good agreement is observed in each case.

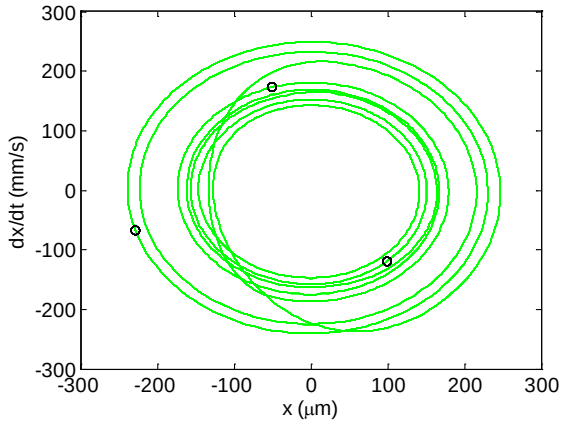

Figure 3(a). Poincaré map for simulated period-3 bifurcation.

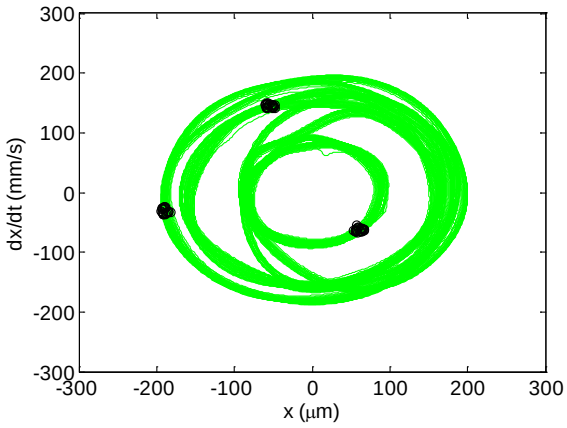

Figure 3(b). Poincaré map for experimental period-3 bifurcation.

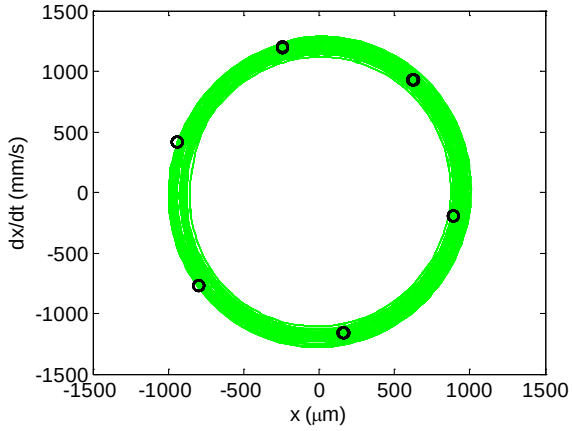

Figure 4(a). Poincaré map for simulated period-6 bifurcation.

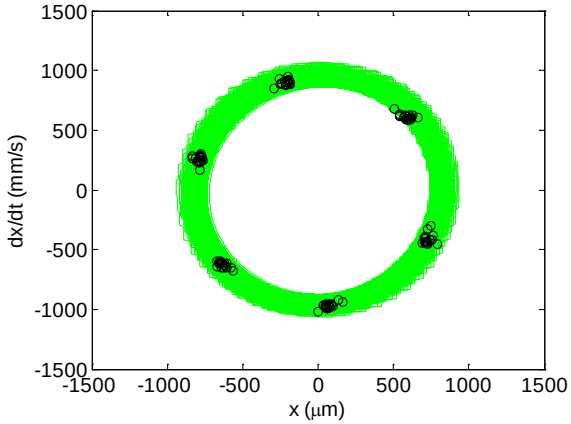

Figure 4(b). Poincaré map for experimental period-6 bifurcation.

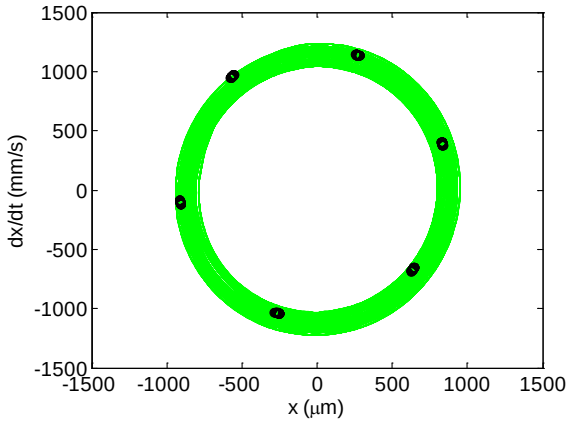

Figure 5(a). Poincaré map for second simulated period-6 bifurcation.

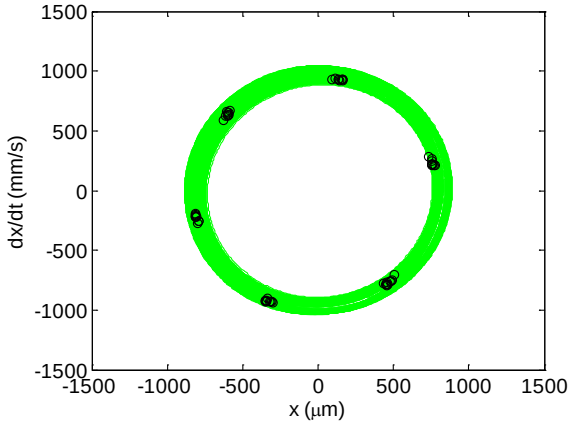

Figure 5(b). Poincaré map for second experimental period-6 bifurcation.

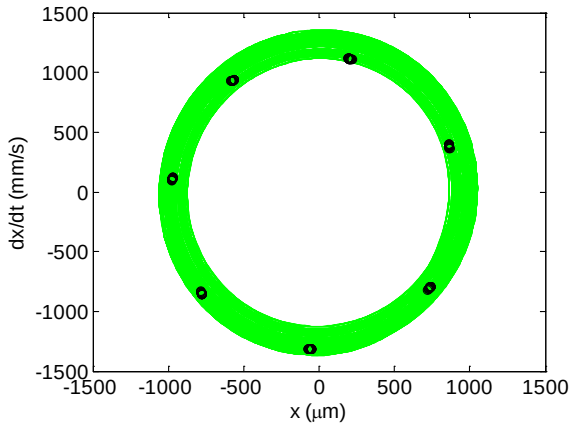

Figure 6(a). Poincaré map for simulated period-7 bifurcation.

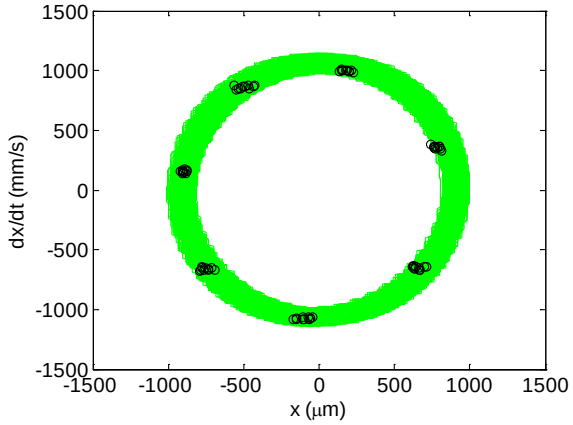

Figure 6(b). Poincaré map for experimental period-7 bifurcation.

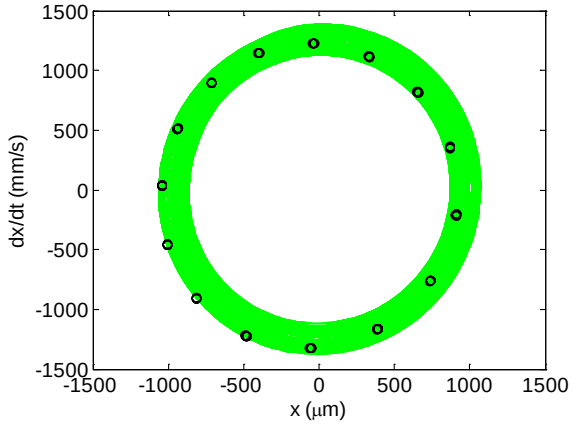

Figure 7(a). Poincaré map for simulated period-15 bifurcation.

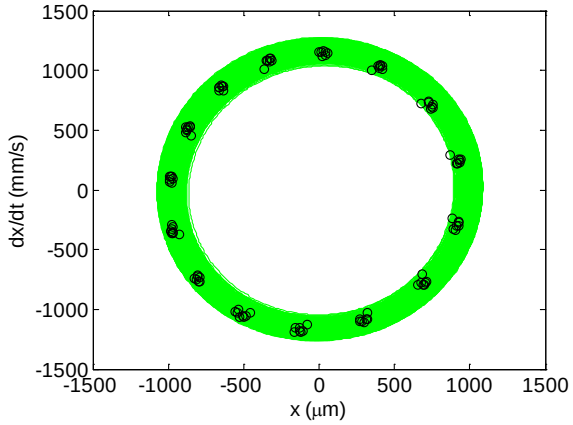

Figure 7(b). Poincaré map for experimental period-15 bifurcation.

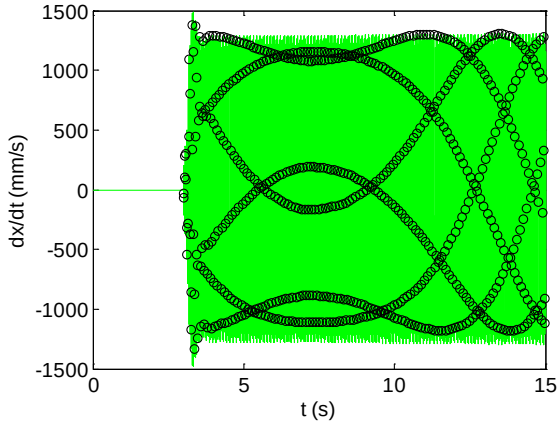

Figure 8(a). Variation in bifurcation behavior with changes in natural frequency for simulated period-6 bifurcation.

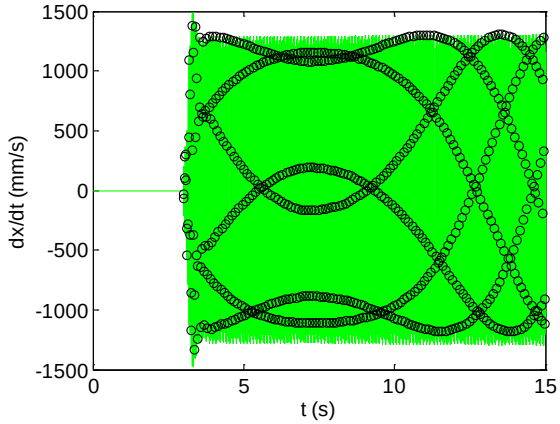

Figure 8(b). Variation in bifurcation behavior with changes in natural frequency for experimental period-6 bifurcation.

Experiments were also completed to demonstrate the sensitivity of the period-n bifurcation behavior to changes in natural frequency. During cutting, material is removed from the workpiece which lowers the workpiece mass and, subsequently, increases the flexure's natural frequency. Since the mass of the chips is much smaller than the workpiece, these changes result in small changes in natural frequency. The changes in system dynamics for the experiments presented in Figs. 8-11 are provided in Table 2. The higher period-n bifurcations exhibited sufficient sensitivity to flexure natural frequency that, within a single cut, both period-n bifurcation and quasi-periodic behavior were observed.

Table 2. Changes in flexure natural frequency due to mass removal.

	Flexure dynamics			
Period -n	Start natural freq.(Hz)	End natural freq. (Hz)	Natural freq. change (Hz)	Mass loss (g)
6	202.4	202.7	0.3	4.8
6	205.7	205.9	0.2	4.1
7	204.1	204.3	0.2	3.9
15	204.7	204.9	0.2	3.7
	Cutting conditions			
Period -n	Spindle speed (rpm)	Axial depth, b (mm)	Radial depth (mm)	
6	3200	18.0	1	
6	3250	15.5	1	
7	3200	14.5	1	
15	3200	14.0	1	

Figures 8-11 show the flexure's feed (x) direction velocity (dx/dt) versus time. The continuous signal is displayed as a solid line, while the circles are the once-per-tooth sampled points. In each figure, (a) shows the simulated behavior and (b) shows the experimental behavior. Good agreement is observed. The time-domain simulation was altered to account for the changing natural frequency due to mass loss. After each time step, the change in mass was calculated based on the volume of the removed chip and the density of the workpiece material. This change in mass was then used to update the flexure's natural frequency for the next time step.

A summary of the behavior seen in Figs. 8-11 is provided here.

1. Figure 8 exhibits period-6 behavior from 4 to 11 s, followed by quasi-periodic behavior until the end of the cut.
2. Figure 9 shows period-6 behavior from 4 to 13 s and then quasi-periodic behavior is observed until the end of the cut.
3. Figure 10 displays quasi-periodic behavior from the beginning of the cut until 11 s and then period-7 behavior from 11 to 15 s.
4. Figure 11 exhibits quasi-periodic behavior from the beginning of the cut until 8 s, period-15 behavior from 8 to 13 s, and then quasi-periodic behavior until the end of the cut

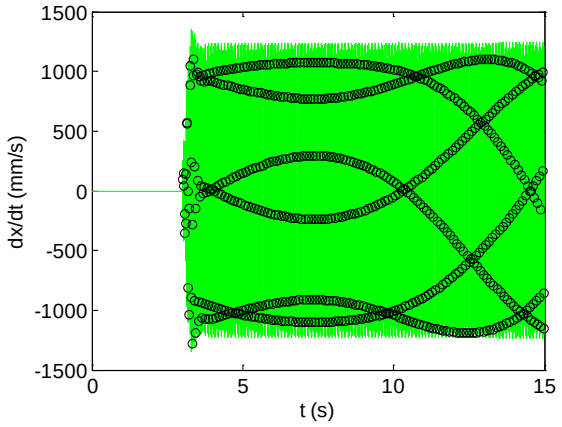

Figure 9(a). Variation in bifurcation behavior with changes in natural frequency for second simulated period-6 bifurcation.

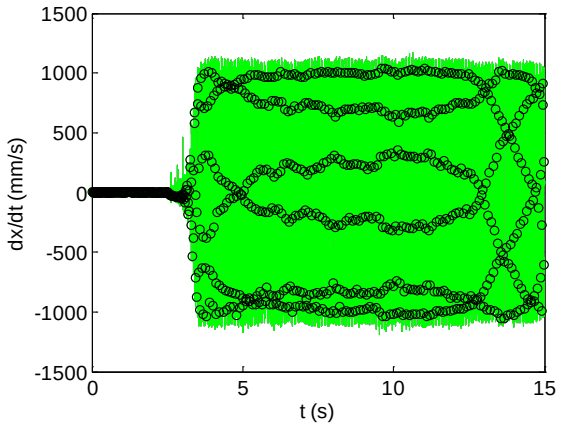

Figure 9(b). Variation in bifurcation behavior with changes in natural frequency for second experimental period-6 bifurcation.

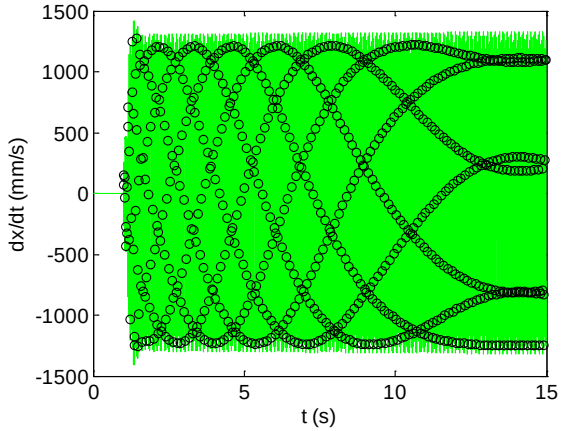

Figure 10(a). Variation in bifurcation behavior with changes in natural frequency for simulated period-7 bifurcation.

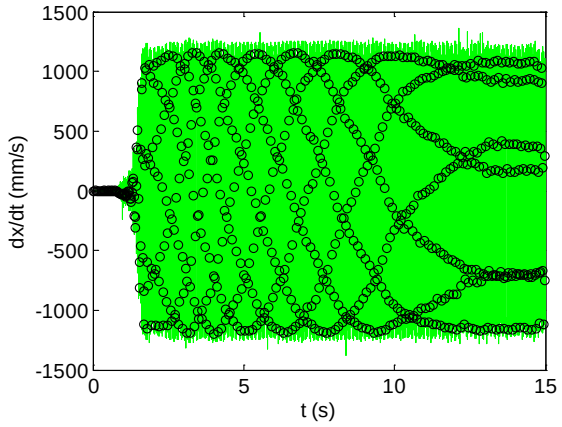

Figure 10(b). Variation in bifurcation behavior with changes in natural frequency for experimental period-7 bifurcation.

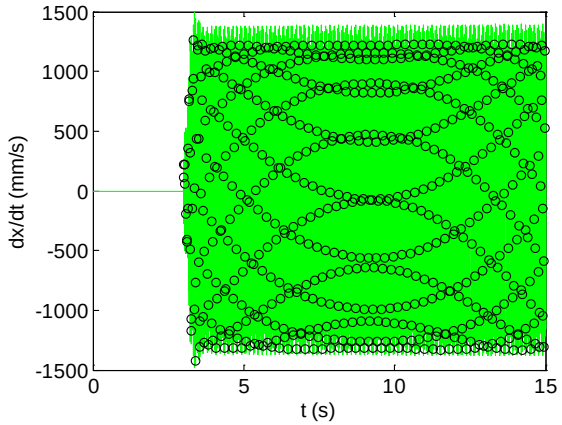

Figure 11(a). Variation in bifurcation behavior with changes in natural frequency for simulated period-15 bifurcation.

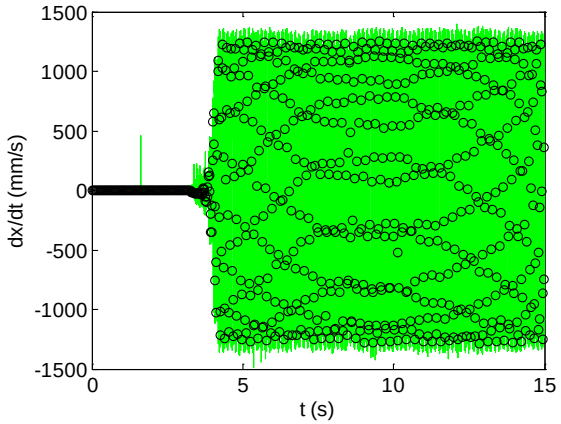

Figure 11(b). Variation in bifurcation behavior with changes in natural frequency for experimental period-15 bifurcation.

REFERENCES

[1] Arnold, R.N., 1946, The mechanism of tool vibration in the cutting of steel, Proceedings of the Institute of Mechanical Engineers, 154.

[2] Doi, S. and Kato, S., 1956, Chatter vibration of lathe tools, Transactions of the ASME, 78: 1127-1134.

[3] Tobias, S.A. and Fishwick, W., 1958, The chatter of lathe tools under orthogonal cutting conditions, Transactions of the ASME, 80: 1079-1088.

[4] Tlusty, J. and Polacek, M., 1963, The stability of machine tools against self-excited vibrations in machining, In: Proceedings of the ASME International Research in Production Engineering Conference, Pittsburgh, PA, 465-474.

[5] Merritt, H.E., 1965, Theory of self-excited machine-tool chatter, ASME Journal of Engineering for Industry, 87: 447-454.

[6] Smith, K.S. and Tlusty, J., 1991, An overview of modeling and simulation of the milling process, Journal of Engineering for Industry, 113: 169-175.

[7] Zhao, M.X. and Balachandran, B., 2001, Dynamics and stability of milling process, International Journal of Solids and Structures, 38: 2233-2248.

[8] Mann, B.P., Insperger, T., Bayly, P.V., and Stépán, G., 2003, Stability of up-milling and down-milling, Part 1: Alternative analytical methods, International Journal of Machine Tools and Manufacture, 43/1: 25-34.

[9] Govekar, E., Gradišek, J., Kalveram, M., Insperger, T., Weinert, K., Stepan, G., and Grabec, I., 2005, On stability and dynamics of milling at small radial immersion, Annals of the CIRP, 54/1: 357-362.

[10] Schmitz, T., and Smith, K.S., 2009, Machining Dynamics: Frequency Response to Improved Productivity, Springer, New York, NY.